**Atmospheric
Measurement
Techniques
Discussions**

First quantitative bias estimates for tropospheric NO_2 columns retrieved from SCIAMACHY, OMI, and GOME-2 using a common standard

H. Irie[1], K. F. Boersma[2,3], Y. Kanaya[4], H. Takashima[4,5], X. Pan[4], and Z. F. Wang[6]

[1]Center for Environmental Remote Sensing, Chiba University, 1-33 Yayoicho, Inage-ku, Chiba 263-8522, Japan
[2]Royal Netherlands Meteorological Institute, Climate Observations Department, P.O. Box 201, 3730 AE De Bilt, The Netherlands
[3]Eindhoven University of Technology, Fluid Dynamics Lab, Eindhoven, The Netherlands
[4]Research Institute for Global Change, Japan Agency for Marine-Earth Science and Technology, 3173-25 Showa-machi, Kanazawa-ku, Yokohama, Kanagawa 236-0001, Japan
[5]Department of Earth System Science, Faculty of Science, Fukuoka University, 8-19-1 Nanakuma, Jounan-ku, Fukuoka 814-0180, Japan
[6]LAPC, Institute of Atmospheric Physics, Chinese Academy of Sciences, Beijing 100029, China

Discussion Paper | Discussion Paper | Discussion Paper | Discussion Paper |

AMTD

5, 3953–3971, 2012

First quantitative bias estimates for tropospheric NO_2 columns

H. Irie et al.

Title Page

Abstract | Introduction

Conclusions | References

Tables | Figures

|◄ | ►|

◄ | ►

Back | Close

Full Screen / Esc

Printer-friendly Version

Interactive Discussion

First quantitative bias estimates for tropospheric NO$_2$ columns

H. Irie et al.

Abstract

For the intercomparison of tropospheric nitrogen dioxide (NO_2) vertical column density (VCD) data from three different satellite sensors (SCIAMACHY, OMI, and GOME-2), we use a common standard to quantitatively evaluate the biases for the respective data sets. As the standard, a regression analysis using a single set of collocated ground-based Multi-Axis Differential Optical Absorption Spectroscopy (MAX-DOAS) observations at several sites in Japan and China in 2006–2011 is adopted. Examination of various spatial coincidence criteria indicates that the slope of the regression line can be influenced by the spatial distribution of NO_2 over the area considered. While the slope varies systematically with the distance between the MAX-DOAS and satellite observation points around Tokyo in Japan, such a systematic dependence is not clearly seen and correlation coefficients are generally higher in comparisons at sites in China. On the basis of these results, we focus mainly on comparisons over China and best estimate the biases in SCIAMACHY, OMI, and GOME-2 data (TM4NO2A and DOMINO version 2 products) against the MAX-DOAS observations to be -5 ± 14 %, -10 ± 14 %, and $+1 \pm 14$ %, respectively, which are all small and insignificant. We suggest that these small biases now allow analyses combining these satellite data for air quality studies that are more systematic and quantitative than previously possible.

1 Introduction

Three satellite sensors, SCIAMACHY (SCanning Imaging Absorption SpectroMeter for Atmospheric CHartographY) (Bovensmann et al., 1999), OMI (Ozone Monitoring Instrument) (Levelt et al., 2006), and GOME-2 (Global Ozone Monitoring Experiment-2) (Callies et al., 2000), were all in orbit together until April 2012, observing tropospheric nitrogen dioxide (NO_2) pollution on global scale and providing long-term data records (since 2002) of vertical column densities (VCDs). Observations by these satellite sensors were performed at different local times, and the diurnal variation pattern seen

Title Page

Abstract | Introduction

Conclusions | References

Tables | Figures

◀ | ▶

◀ | ▶

Back | Close

Full Screen / Esc

Printer-friendly Version

Interactive Discussion

in the NO_2 data has been reported for various locations over the world (Boersma et al., 2008). However, the diurnal cycle observed by SCIAMACHY and OMI has been validated only over the Middle East, a region with highly active photochemistry (Boersma et al., 2009). The observations of the diurnal variation are expected to provide additional constraints to improve models, beyond a single VCD data set at a specific local time (e.g., Lin et al., 2010). The combined use of SCIAMACHY, OMI, and GOME-2 data is desirable to improve our understanding of short-term variations in chemistry, emissions and transport of pollution. There have been, however, few studies attempting to quantify the biases in SCIAMACHY, OMI, and GOME-2 data in a consistent manner based on comparisons with independent observations. In East Asia, even validation comparisons for a specific satellite data set are very limited, except for the NASA OMI standard product (Irie et al., 2009). Here we present such a consistent data set based on Multi-Axis Differential Optical Absorption Spectroscopy (MAX-DOAS) observations performed at several sites in Japan and China in 2006–2011. Because MAX-DOAS provides continuous measurements during daytime, its data are used as a common reference to validate all three satellite data sets.

2 Satellite observations

The present study targets tropospheric NO_2 VCD data from SCIAMACHY, OMI, and GOME-2, all of which are equipped with a UV/visible sensor measuring sunlight backscattered from the Earth's atmosphere and reflected by the surface as well as the direct solar irradiance spectrum. SCIAMACHY was launched onboard the ENVISAT satellite in March 2002. It passes over the equator at about 10:00 LT and achieves global coverage observations in six days, with a spatial resolution of $60 \times 30\,km^2$. OMI was launched onboard the Aura satellite in July 2004. The equator crossing time is about 13:40–13:50 LT. Daily global measurements are achieved by a wide field of view (FOV) of 114°, in which 60 discrete viewing angles (at a nominal nadir spatial resolution of $13 \times 24\,km^2$) are distributed perpendicular to the flight direction. The GOME-2

First quantitative bias estimates for tropospheric NO$_2$ columns

H. Irie et al.

Title Page

Abstract | Introduction

Conclusions | References

Tables | Figures

◄ | ►|

◄ | ►

Back | Close

Full Screen / Esc

Printer-friendly Version

Interactive Discussion

instrument, launched aboard a MetOp satellite in June 2006, has a ground-pixel size of 80×40 km^2 (240×40 km^2 for the back scan) over most of the globe. With its wide swath, near-global coverage (with an equator crossing time around 09:30 LT) is achieved every day. While observation specifications are thus somewhat different between the three sensors, tropospheric NO$_2$ VCD data retrieved with the same basic algorithm (DOMINO products for OMI and TM4NO2A products for SCIAMACHY and GOME-2) (Boersma et al., 2004, 2007, 2011) are compared in detail with MAX-DOAS data below. The error in the satellite tropospheric NO$_2$ VCD data includes uncertainties in the slant column, the stratospheric column, and the tropospheric air mass factor (AMF) (Boersma et al., 2004), and can be expressed as $\sim 1 \times 10^{15}$ molecules cm^{-2} + 30 % for polluted situations. Comparisons are made for the version 2 retrievals under cloud-free conditions, i.e. cloud fraction (CF) less than 20 %.

3 MAX-DOAS observations

Here we briefly describe ground-based MAX-DOAS measurements – scattered sunlight observations in the UV/visible at several elevation angles between the horizon and zenith (e.g., Hönninger and Platt, 2002; Hönninger et al., 2004) – performed at three sites in Japan and three sites in China (Table 1 and Fig. 1). As can be seen in Fig. 1, the MAX-DOAS measurements were conducted at various levels of NO$_2$ pollution, covering urban (Yokosuka), suburban (Tsukuba) around Tokyo, and remote areas (Hedo) in Japan and the northernmost (Mangshan), middle (Tai'an), and southernmost (Rudong) parts of the highly polluted area in China. This set of observations extends the data set used by Irie et al. (2009) for the validation of the NASA OMI NO$_2$ standard product. The present study additionally uses data for 2009–2011 and data from the Mangshan and Rudong sites. The observations at Tai'an, Mangshan, and Rudong were made as part of intensive observation campaigns for a limited time period of about 1 month for each site (Table 1). The instrumentation and retrieval algorithm used for all the sites have been described in detail elsewhere (e.g., Irie et al., 2008, 2009, 2011; Takashima

et al., 2011a, 2011b). The retrieval utilizes absorption features by NO$_2$ and the oxygen dimer (O$_4$) at 460–490 nm. The NO$_2$ absorption cross section data of Vandaele et al. (1998) at 294 K were used. The quality of our DOAS analysis is supported by formal semi-blind intercomparison results indicating good agreement with other MAX-DOAS observations to within ~10 % of other instruments for both NO$_2$ and O$_4$ differential slant column densities (ΔSCD) and for both the UV and visible regions (Roscoe et al., 2010). The O$_4$ ΔSCD values derived from the DOAS analysis are converted using our aerosol retrieval algorithm (e.g., Irie et al., 2008) to aerosol optical depth and the vertical profile of the aerosol extinction coefficient. At the same time, the so-called box AMF is uniquely determined, as it is a function of the aerosol profile. Using this AMF information and a nonlinear iterative inversion method, the NO$_2$ΔSCD values are converted to the tropospheric VCD and the vertical profile of NO$_2$. Error analysis for the retrieved NO$_2$ VCDs has been done based on the method described by Irie et al. (2011). For an NO$_2$ VCD of about 100×10^{14} molecules cm^{-2}, typical random errors were estimated to be 5×10^{14} molecules cm^{-2} (5 %). Systematic errors due to uncertainty in the AMF determination, which is likely the dominant source of systematic error in our profile retrieval method, were estimated to be 7×10^{14} molecules cm^{-2} (7 %). For the present study, additional sensitivity analysis is performed using a different fitting window for NO$_2$ (425–450 nm) and different NO$_2$ cross section data (at 220 K). The errors were estimated by a manner similar to Takashima et al. (2011b) to be about −3 % (the VCD retrieved from 425–450 nm is smaller) and −23 % (the VCD retrieved using the cross section at 220 K is smaller). Scaling the latter estimate to the actual temperature variation below 2 km (possibly cooled down to ~260 K at an altitude of 2 km) yields −11 %. This value could be smaller, since NO$_2$ should be abundant near the surface, where the temperature is usually warmer than 260 K and occasionally can exceed 294 K. However, we quantified the overall uncertainty to be 14 % as the root-mean squares of all the above estimated errors. The representative horizontal distance for air masses observed by MAX-DOAS was estimated to be about 10 km (Irie et al., 2011), a magnitude comparable to or better than the satellite observations. The temporal resolution was

30 min, which corresponds to a complete sequence of elevation angles. In the present study, a comparison is made only when the time difference between MAX-DOAS and satellite observations was less than 30 min.

4   Results and discussion

Here we compare MAX-DOAS observations performed in Japan and China in 2006–2011 with all three types of satellite products in a consistent manner. In Fig. 2, comparisons between MAX-DOAS and OMI tropospheric NO_2 column data are made only if the center of the OMI pixel is within 0.20° latitude and longitude of an MAX-DOAS observation point. This coincidence criterion is hereinafter denoted x. Two regression lines are shown in Fig. 2. The one shown in blue has been drawn from comparisons for Tsukuba, Yokosuka, and Hedo. The regression line shown in red was obtained from comparisons for three Chinese sites (Tai'an, Mangshan, and Rudong) and Hedo. The respective cases are called hereafter the Tokyo case and China case. The slopes for the Tokyo cases are controlled mainly by comparisons over Tsukuba and Yokosuka, which are both located around Tokyo, and for the China case the three Chinese sites, as their data are distributed over a wide range of NO_2 value. For comparisons over Hedo (shown in green), which is located in a remote area, both satellite and MAX-DOAS data show reasonable, very small NO_2 VCD values, compared to the other sites. The same features were seen for all the other cases investigated in this study. Considering this, the regression analysis has been made with the intercept forced to be zero, in order to simplify the interpretation of changes in the bias estimated from the slope of the regression line under various conditions.

In Fig. 2, we find excellent agreement for the China case; the slope (± its 1σ standard deviation) is almost unity at 1.03 ± 0.02. On the other hand, the slope for the Tokyo case is only 0.63 ± 0.01. For both cases, correlation coefficients (R^2) are as high as 0.78 and 0.69, respectively.

To investigate the cause of the difference, we make comparisons with various coincidence criteria. We test 15 different coincidence criteria: $x = 0.05°$, $0.10°$, $0.15°$, $0.20°$, $0.25°$, $0.30°$, $0.35°$, $0.40°$, $0.45°$, $0.50°$, $0.60°$, $0.70°$, $0.80°$, $0.90°$, and $1.00°$. The results for $x = 0.40°$, $0.60°$, and $1.00°$ are highlighted in Fig. 3. Variations of the slope and R^2
over x are summarized in Figs. 4 and 5 for the Tokyo and China cases, respectively.

For the Tokyo case, we find that the slopes of the regression lines tend to be smaller when a looser coincidence criterion is used, for all comparisons with SCIAMACHY, OMI, and GOME-2. As can be seen in Fig. 1, tropospheric NO_2 VCD values in the surrounding areas of Yokosuka and Tsukuba sites usually drop quickly, owing to limited NOx source regions. For a larger x, there is a higher probability that the satellite footprints include clean air masses, and this tends to lower both the slope and R^2 (Fig. 4). The Yokosuka site is surrounded by industrial facilities, ocean (Tokyo Bay), heavy ship activity, etc., resulting in a large range of tropospheric NO_2 VCD but more scatter in the correlation, compared to the Tsukuba data (Figs. 2 and 3). To better address such influences of spatial inhomogeneity in a satellite pixel, validation observations covering several points in a satellite pixel at the same time would be desirable (e.g., Piters et al., 2012).

In Fig. 5, results of the estimated slopes and R^2 for the China case are shown. Results with an insufficient number of comparisons (less than 3) at Chinese sites have been omitted. It can be seen that the slopes slowly vary with x but the variations are not as systematic as those of the Tokyo case. R^2 values are greater than 0.6 for all comparisons and usually higher than those for the Tokyo case (Figs. 4 and 5). These suggest that the spatial distributions of tropospheric NO_2 VCDs around the Chinese sites during the observation periods were rather homogeneous and therefore appropriate for bias estimates.

All the slopes estimated from comparisons over China range from 0.8 to 1.2. By simply averaging the slopes over the entire x range, the biases with respect to MAX-DOAS observations are estimated to be $0 \pm 14\%$, $-8 \pm 14\%$, and $-10 \pm 14\%$ for SCIA-MACHY, OMI, and GOME-2, respectively (Table 2). The error of $\pm 14\%$ is due mostly

to the uncertainty in the MAX-DOAS NO_2 retrieval, as mentioned above. It is expected, however, that the validation comparison can be more precise using a stricter coincidence criterion owing to the increased probability of observing the same air masses by a satellite sensor and MAX-DOAS. Considering this, our best estimates of the biases from slopes at a strict x range below $0.50°$ are $-5 \pm 14\%$, $-10 \pm 14\%$, and $+1 \pm 14\%$ for SCIAMACHY, OMI, and GOME-2, respectively (Table 2). Thus, our study confirms the hypothesized high-quality KNMI products retrieved with the new method of Boersma et al. (2011).

5 Conclusions

To quantify the biases in the tropospheric NO_2 VCD data from SCIAMACHY, OMI, and GOME-2 in a consistent manner, we created a single data set from MAX-DOAS observations performed at three sites in Japan and three sites in China in 2006–2011. Regression analysis between satellite and MAX-DOAS tropospheric NO_2 VCDs showed that the slope of the regression line tends to be biased by the distance between MAX-DOAS and satellite observation points, due to a difference in the spatial representativeness between MAX-DOAS and satellite observations under loose coincidence criteria. This feature is more clearly seen around Tokyo with strong spatial gradients in air pollution. These results serve as a guideline for future satellite validation, in terms of the choice of coincidence criteria and validation sites. We recommend conducting validation observations under relatively homogeneously polluted conditions. From the slopes of the regression lines for strict coincidence criteria, we estimated biases in SCIAMACHY, OMI, and GOME-2 data to be $-5 \pm 14\%$, $-10 \pm 14\%$, and $+1 \pm 14\%$, respectively, compared to the MAX-DOAS data. Thus, we conclude that the biases are less than about 10% and insignificant for all three data sets. Thus, with a consideration of these characteristics, the present study encourages the combination of these satellite data to realize air quality studies that are more systematic and quantitative than previously possible.

References

Boersma, K. F., Eskes, H. J., and Brinksma, E. J.: Error Analysis for tropospheric NO_2 retrieval from space, J. Geophys. Res., 109, D04311, doi:10.1029/2003JD003962, 2004.

Boersma, K. F., Eskes, H. J., Veefkind, J. P., Brinksma, E. J., van der A, R. J., Sneep, M., van den Oord, G. H. J., Levelt, P. F., Stammes, P., Gleason, J. F., and Bucsela, E. J.: Near-real time retrieval of tropospheric NO_2 from OMI, Atmos. Chem. Phys., 7, 2103–2118, doi:10.5194/acp-7-2103-2007, 2007.

Boersma, K. F., Jacob, D. J., Eskes, H. J., Pinder, R. W., Wang, J., and van der A, R. J.: Intercomparison of SCIAMACHY and OMI tropospheric NO_2 columns: Observing the diurnal evolution of chemistry and emissions from space, J. Geophys. Res., 113, D16S26, doi:10.1029/2007JD008816, 2008.

Boersma, K. F., Jacob, D. J., Trainic, M., Rudich, Y., DeSmedt, I., Dirksen, R., and Eskes, H. J.: Validation of urban NO_2 concentrations and their diurnal and seasonal variations observed from the SCIAMACHY and OMI sensors using in situ surface measurements in Israeli cities, Atmos. Chem. Phys., 9, 3867–3879, doi:10.5194/acp-9-3867-2009, 2009.

Boersma, K. F., Eskes, H. J., Dirksen, R. J., van der A, R. J., Veefkind, J. P., Stammes, P., Huijnen, V., Kleipool, Q. L., Sneep, M., Claas, J., Leitã o, J., Richter, A., Zhou, Y., and Brunner, D.: An improved tropospheric NO_2 column retrieval algorithm for the Ozone Monitoring Instrument, Atmos. Meas. Tech., 4, 1905–1928, doi:10.5194/amt-4-1905-2011, 2011.

Bovensmann, H., Burrows, J. P., Buchwitz, M., Frerick, J., Noel, S., Rozanov, V. V., Chance, K. V., and Goede, A. H. P.: SCIAMACHY – Mission objectives and measurement modes, J. Atmos. Sci., 56, 127–150, doi:10.1175/1520-0469(1999)056¡0127:SMOAMM¿2.0.CO;2, 1999.

Callies, J., Corpaccioli, E., Eisinger, M., Hahne, A., and Lefebvre, A.: GOME-2- Metop's second-generation sensor for operational ozone monitoring, ESA Bull., 102, 28–36, 2000.

Title Page

Abstract | Introduction

Conclusions | References

Tables | Figures

Back | Close

Full Screen / Esc

Printer-friendly Version

Interactive Discussion

Hönninger, G. and Platt, U.: Observations of BrO and its vertical distribution during surface ozone depletion at Alert, Atmos. Environ., 36, 2481–2489, 2002.

Hönninger, G., von Friedeburg, C., and Platt, U.: Multi axis differential optical absorption spectroscopy (MAX-DOAS), Atmos. Chem. Phys., 4, 231–254, doi:10.5194/acp-4-231-2004, 2004.

Irie, H., Kanaya, Y., Akimoto, H., Iwabuchi, H., Shimizu, A., and Aoki, K.: First retrieval of tropospheric aerosol profiles using MAX-DOAS and comparison with lidar and sky radiometer measurements, Atmos. Chem. Phys., 8, 341–350, doi:10.5194/acp-8-341-2008, 2008.

Irie, H., Kanaya, Y., Takashima, H., Gleason, J. F., and Wang, Z.: Characterization of OMI tropospheric NO_2 measurements in East Asia based on a robust validation comparison, SOLA, 5, 117–120, doi:10.2151/sola.2009-030, 2009.

Irie, H., Takashima, H., Kanaya, Y., Boersma, K. F., Gast, L., Wittrock, F., Brunner, D., Zhou, Y., and Van Roozendael, M.: Eight-component retrievals from ground-based MAX-DOAS observations, Atmos. Meas. Tech., 4, 1027–1044, doi:10.5194/amt-4-1027-2011, 2011.

Levelt, P. F., van den Oord, G. H. J., Dobber, M. R., Malkki, A., Visser, H., de Vries, J., Stammes, P., Lundell, J., and Saari, H.: The Ozone Monitoring Instrument, IEEE, Trans. Geo. Rem. Sens., 44, 5, 1093–1101, doi:10.1109/TGRS.2006.872333, 2006.

Lin, J.-T., McElroy, M. B., and Boersma, K. F.: Constraint of anthropogenic NO_x emissions in China from different sectors: a new methodology using multiple satellite retrievals, Atmos. Chem. Phys., 10, 63–78, doi:10.5194/acp-10-63-2010, 2010.

Piters, A. J. M., Boersma, K. F., Kroon, M., Hains, J. C., Van Roozendael, M., Wittrock, F., Abuhassan, N., Adams, C., Akrami, M., Allaart, M. A. F., Apituley, A., Beirle, S., Bergwerff, J. B., Berkhout, A. J. C., Brunner, D., Cede, A., Chong, J., Clémer, K., Fayt, C., Frieß, U., Gast, L. F. L., Gil-Ojeda, M., Goutail, F., Graves, R., Griesfeller, A., Großmann, K., Hemerijckx, G., Hendrick, F., Henzing, B., Herman, J., Hermans, C., Hoexum, M., van der Hoff, G. R., Irie, H., Johnston, P. V., Kanaya, Y., Kim, Y. J., Klein Baltink, H., Kreher, K., de Leeuw, G., Leigh, R., Merlaud, A., Moerman, M. M., Monks, P. S., Mount, G. H., Navarro-Comas, M., Oetjen, H., Pazmino, A., Perez-Camacho, M., Peters, E., du Piesanie, A., Pinardi, G., Puentedura, O., Richter, A., Roscoe, H. K., Schönhardt, A., Schwarzenbach, B., Shaiganfar, R., Sluis, W., Spinei, E., Stolk, A. P., Strong, K., Swart, D. P. J., Takashima, H., Vlemmix, T., Vrekoussis, M., Wagner, T., Whyte, C., Wilson, K. M., Yela, M., Yilmaz, S., Zieger, P., and Zhou, Y.: The Cabauw Intercomparison campaign for Nitrogen Dioxide measuring Instruments (CINDI):

First quantitative bias estimates for tropospheric NO_2 columns

H. Irie et al.

Title Page

Abstract | Introduction

Conclusions | References

Tables | Figures

◄ | ►

◄ | ►

Back | Close

Full Screen / Esc

Printer-friendly Version

Interactive Discussion

design, execution, and early results, Atmos. Meas. Tech., 5, 457–485, doi:10.5194/amt-5-457-2012, 2012.

Roscoe, H. K., Van Roozendael, M., Fayt, C., du Piesanie, A., Abuhassan, N., Adams, C., Akrami, M., Cede, A., Chong, J., Clémer, K., Friess, U., Gil Ojeda, M., Goutail, F., Graves, R., Griesfeller, A., Grossmann, K., Hemerijckx, G., Hendrick, F., Herman, J., Hermans, C., Irie, H., Johnston, P. V., Kanaya, Y., Kreher, K., Leigh, R., Merlaud, A., Mount, G. H., Navarro, M., Oetjen, H., Pazmino, A., Perez-Camacho, M., Peters, E., Pinardi, G., Puentedura, O., Richter, A., Schönhardt, A., Shaiganfar, R., Spinei, E., Strong, K., Takashima, H., Vlemmix, T., Vrekoussis, M., Wagner, T., Wittrock, F., Yela, M., Yilmaz, S., Boersma, F., Hains, J., Kroon, M., Piters, A., and Kim, Y. J.: Intercomparison of slant column measurements of NO_2 and O_4 by MAX-DOAS and zenith-sky UV and visible spectrometers, Atmos. Meas. Tech., 3, 1629–1646, doi:10.5194/amt-3-1629-2010, 2010.

Takashima, H., Irie, H., Kanaya, Y., and Akimoto, H.: Enhanced NO_2 at Okinawa Island, Japan caused by rapid air-mass transport from China as observed by MAX-DOAS, Atmos. Environ., 45, 2593–2597, 2011a.

Takashima, H., Irie, H., Kanaya, Y., and Syamsudin, F.: NO_2 observations over the western Pacific and Indian Ocean by MAX-DOAS on Kaiyo, a Japanese research vessel, Atmos. Meas. Tech. Discuss., 4, 6069–6095, doi:10.5194/amtd-4-6069-2011, 2011b.

Vandaele, A. C., Hermans, C., Simon, P. C., Carleer, M., Colin, R., Fally, S., Mérienne, M. F., Jenouvrier, A., and Coquart, B.: Measurements of the NO_2 absorption cross-section from 42000 cm^{-1} to 10000 cm^{-1} (238–1000 nm) at 220 K and 294 K, J. Quant. Spectrosc. Ra., 59, 171–184, doi:10.1016/S0022-4073(97)00168-4, 1998.

Title Page

Abstract | Introduction

Conclusions | References

Tables | Figures

|◄ | ►|

◄ | ►

Back | Close

Full Screen / Esc

Printer-friendly Version

Interactive Discussion

First quantitative bias estimates for tropospheric NO$_2$ columns

H. Irie et al.

Table 1. Site information for MAX-DOAS observations.

Site	Location	Period[a]	N_{total}^b
Tsukuba	36.05° N, 140.12° E	1 Nov 2006–16 Mar 2007	1005
		1 Jun 2010–31 Dec 2011	5146
Hedo	26.87° N, 128.25° E	30 Mar 2007–31 Dec 2011	16 682
Yokosuka	35.32° N, 139.65° E	30 Mar 2007–31 Dec 2011	14 708
Tai'an	36.16° N, 117.15° E	28 May–29 Jun 2006	333
Mangshan	40.26° N, 116.28° E	7 Sep–6 Oct 2007	165
Rudong	32.26° N, 121.37° E	14 May–23 Jun 2010	669[c]

[a] Measurements were not always made continuously in the period, for example, due to cloudy conditions.
[b] The total number of NO$_2$ VCD data points available in the period.
[c] For two MAX-DOAS instruments directed to different azimuth angles.

H. Irie et al.

Table 2. Estimated biases in satellite tropospheric NO$_2$ products for different coincidence criterion thresholds.

Sensor	$x \leq 0.5°$	$x \leq 1.0°$
SCIAMACHY	$-5 \pm 14\%$	$0 \pm 14\%$
OMI	$-10 \pm 14\%$	$-8 \pm 14\%$
GOME-2	$+1 \pm 14\%$	$-10 \pm 14\%$

H. Irie et al.
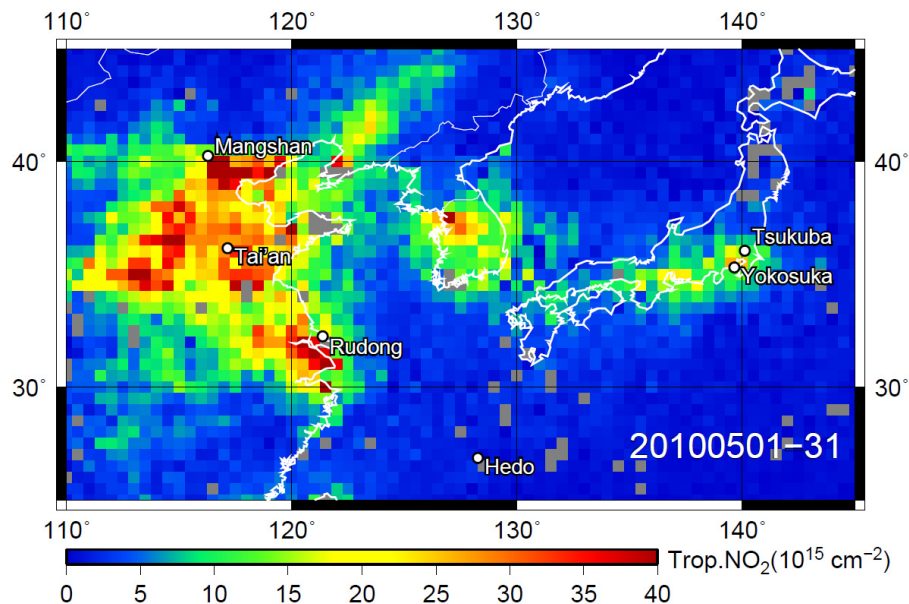
Fig. 1. Locations of MAX-DOAS observations on a monthly mean map (0.5° grid) of GOME-2 tropospheric NO$_2$ VCD data in May 2010.
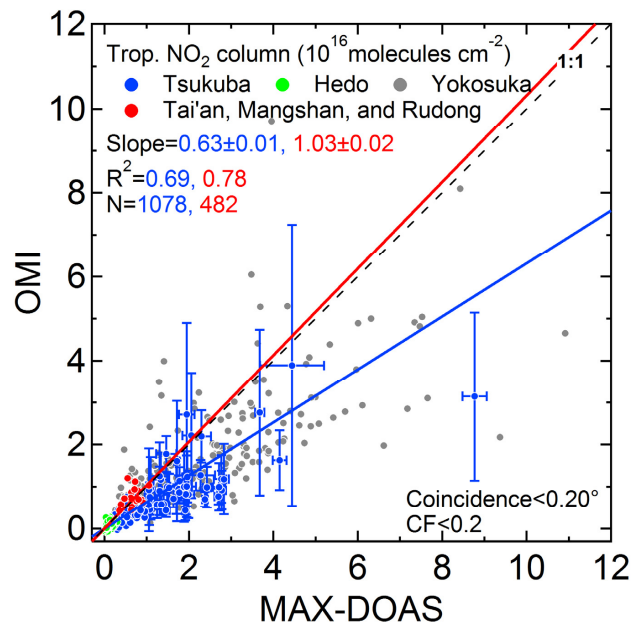
Fig. 2. Correlations between tropospheric NO_2 VCDs (10^{16} molecules cm^{-2}) from OMI and MAX-DOAS observations at a coincidence criterion (x) of 0.20°. Comparisons over Tsukuba, Hedo, and Yokosuka are shown in blue, green, and gray, respectively, and campaign-based short-term observations in China are shown in red. Error bars for both OMI and MAX-DOAS data are shown only for comparisons over Tsukuba at MAX-DOAS NO_2 VCDs larger than 1×10^{16} molecules cm^{-2}, for clarity. Linear regression analysis has been performed for the respective cases 1 (Tokyo case; blue) and 2 (Chinese case; red), where the slopes of their regression lines are constrained mainly by comparisons made around Tokyo (Tsukuba and Yokosuka) and at China sites (Tai'an, Mangshan, Rudong), respectively. Hedo data are used in both regression analyses but do not constrain the slope much, since the comparisons at other sites are made over a wide range of NO_2 VCD values. For each case, the slope, correlation coefficient (R^2), and number of data points (N) are given in the plot.

Title Page

Abstract | Introduction

Conclusions | References

Tables | Figures

◄ | ►|

◄ | ►

Back | Close

Full Screen / Esc
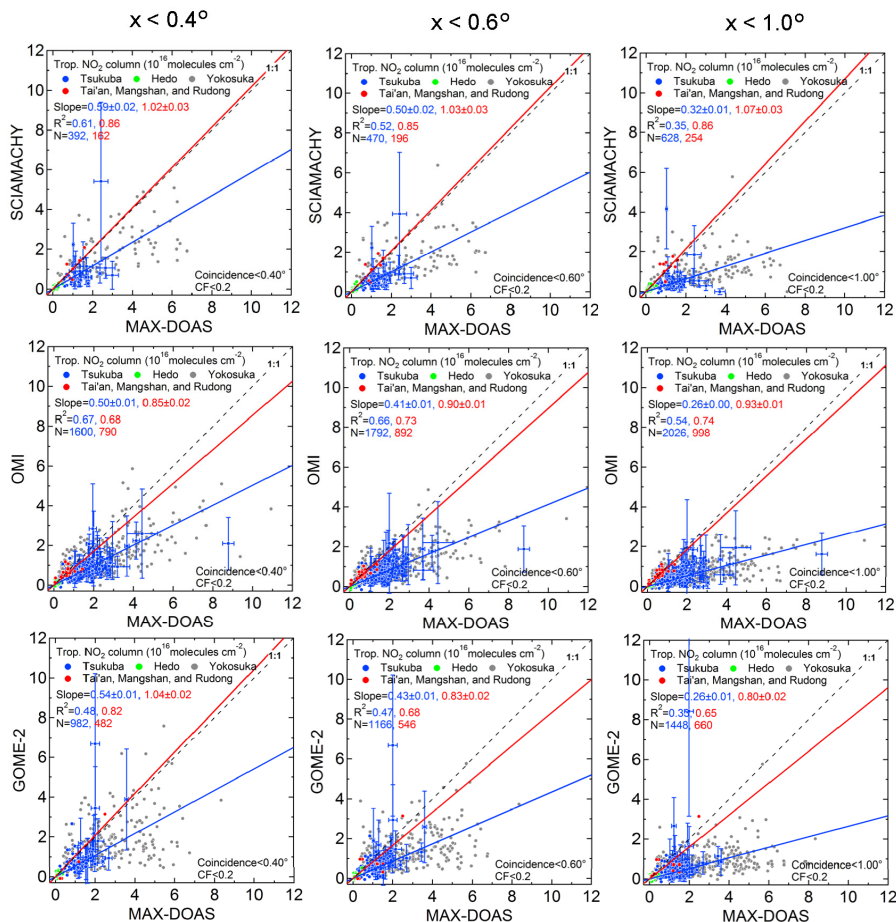
Printer-friendly Version

Interactive Discussion

Fig. 3. Same as Fig. 2 but the first, second, and third rows are for SCIAMACHY, OMI, and GOME-2, respectively. For each satellite sensor, three plots using different coincidence criteria (*x*) of 0.40°, 0.60°, and 1.00°, with MAX-DOAS are given.
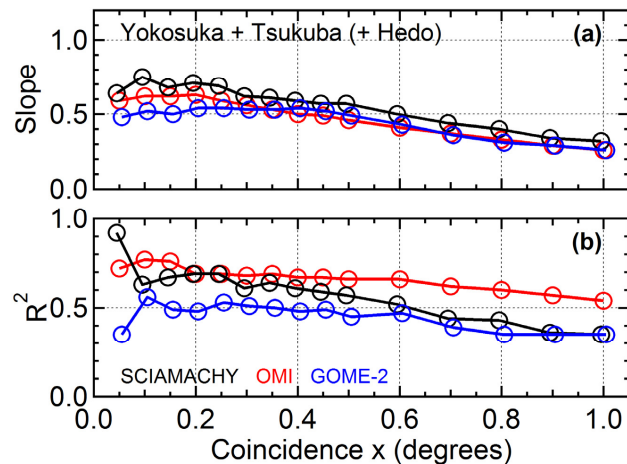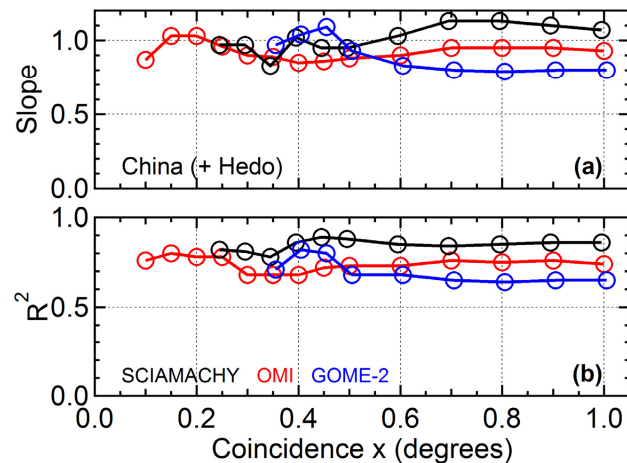
Fig. 4. (a) Slopes and **(b)** R^2 of the regression lines as a function of coincidence criterion x between satellite and MAX-DOAS observations for case 1 (Tokyo case)

Fig. 5. Same as Fig. 4 but for case 2 (China case).